Acoustic distribution of discriminated micronektonic organisms from a bi-frequency processing: the case study of eastern Kerguelen oceanic waters

Nolwenn Béhagle, Cédric Cotté, Anne Lebourges-Dhaussy, Gildas Roudaut, Guy Duhamel, Patrice Brehmer, Erwan Josse, Yves Cherel

Acoustic distribution of discriminated micronektonic organisms from a bi-frequency processing: the case study of eastern Kerguelen oceanic waters

Nolwenn Béhagle[a,b*], Cédric Cotté[c], Anne Lebourges-Dhaussy[a], Gildas Roudaut[a], Guy Duhamel[d], Patrice Brehmer[e], Erwan Josse[a], Yves Cherel[f]

[a]*IRD, UMR LEMAR 6539 (CNRS-IRD-IFREMER-UBO), BP70, 29280 Plouzané, France*

[b]*CNRS, UMR LOCEAN 7159 (CNRS-IRD-MNHN-UPMC), 4 place Jussieu, 75005 Paris, France*

[c]*MNHN, UMR LOCEAN 7159 (CNRS-IRD-MNHN-UPMC), 4 place Jussieu, 75005 Paris, France*

[d]*MNHN, UMR BOREA 7208(MNHN- CNRS-UPMC-IRD-UCBN-UAG), 43 rue Cuvier, CP 26,75231 Paris Cedex 05, France*

[e]*IRD, UMR 195 Lemar, ISRA-CRODT, Pole de Recherche de Hann, BP221, Dakar, Sénégal*

[f]*CNRS, UMR CEBC 7372 (CNRS-Université de La Rochelle), 79360 Villiers-en-Bois, France*

[*]Corresponding author. *E-mail address:* nolwenn.behagle@gmail.com

Abstract

Despite its ecological importance, micronekton remains one of the least investigated components of the open-ocean ecosystems. Our main goal was to characterize micronektonic organisms using bi-frequency acoustic data (38 and 120 kHz) by calibrating an algorithm tool that discriminates groups of scatterers in the top 300 m of the productive oceanic zone east of Kerguelen Islands (Indian sector of the Southern Ocean). The bi-frequency algorithm was calibrated from acoustic properties of mono-specific biological samples collected with trawls, thus allowing to discriminate three acoustic groups of micronekton: (*i*) "gas-bearing" ($\Delta S_{v,120-38} < -1$ dB), (*ii*) "fluid-like" ($\Delta S_{v,120-38} > 2$ dB), and (*iii*) "undetermined" scatterers ($-1 < \Delta S_{v,120-38} < 2$ dB). The three groups likely correspond biologically to gas-filled swimbladder fish (myctophids), crustaceans (euphausiids and hyperiid amphipods), and other marine organisms potentially present in these waters and containing either lipid-filled or no inclusion (*e.g.* other myctophids), respectively. The Nautical Area Scattering Coefficient (NASC) was used (echo-integration cells of 10m long and 1m deep) between 30 and 300m depth as a proxy of relative biomass of acoustic targets. The distribution of NASC values showed a complex pattern according to: (*i*) the three acoustically-defined groups, (*ii*) the type of structures (patch *vs.* layers) and (*iii*) the timing of the day (day/night cycle). NASC values were higher at night than during the day. A large proportion of scatterers occurred in layers while patches, that mainly encompass gas-bearing organisms, are especially observed during daytime. This method provided an essential descriptive baseline of the spatial distribution of micronekton and a relevant approach to (*i*) link micronektonic group to physical parameters to define their habitats, (*ii*) investigate trophic interactions by combining active acoustic and top predator satellite tracking, and (*iii*) study the functioning of the pelagic ecosystems at various spatio-temporal scales.

Keywords: Euphausiid, Kerguelen, Myctophid, Southern Ocean, Acoustics.

1. Introduction

Micronektonic organisms (~1-20 cm in length; Kloser et al., 2009) constitute one of the most noticeable and ecologically important components of the open ocean. They amount to a substantial biomass (*e.g.* estimated at > 10 000 million metric tons of mesopelagic fish in oceanic waters worldwide and ~380 million metric tons of Antarctic krill in the Southern Ocean; Atkinson et al., 2009; Irigoien et al., 2014) with high nutritional value (Shaviklo and Rafipour, 2013; Koizumi et al., 2014) leading to increasing commercial interest (Pauly et al., 1998). In oceanic waters, micronekton contribute to the export of carbon from the surface to deeper layers (the biological pump) through extensive daily vertical mesopelagic migrations to feed on near-surface organisms at night (Bianchi et al., 2013). They play a prominent role in oceanic food webs by linking primary consumers to higher predators, including commercially targeted fish species and oceanic squids, together with charismatic species, such as marine mammals and seabirds (Rodhouse and Nigmatullin, 1996; Robertson and Chivers, 1997; Potier et al. 2007; Spear et al. 2007). Despite their ecological importance, micronekton remain one of the least investigated components of the marine ecosystems, with major gaps in our knowledge of their biology, ecology, and major uncertainties about their global biomass (Handegard et al., 2013; Irigoien et al., 2014).

Acoustic methods have been used in fishery operations and research since 1935 (Sund, 1935). Stock assessment drove a continuous improvement of the methods in order to better investigate the distribution and abundance of targeted marine organisms (Simmonds and MacLennan, 2005). Beyond stock assessment, acoustics now extends to whole marine ecosystems, being the best available tool allowing simultaneous collection of qualitative and quantitative data on their biotic and even abiotic components (Bertrand et al., 2013). A major limitation of acoustics is the lack of accurate taxonomic information about the ensonified

70 organisms. Hence, acoustic analytical tools to determine characteristics of biological
71 backscatters were developed by comparing and quantifying the difference of mean volume
72 backscattering strength between different frequencies. The rationale is that the acoustic
73 properties of individual species are known to vary with the operating frequencies of the echo
74 sounder. For example, both experimental and theoretical studies showed large variations in
75 the average echo energy per unit biomass due to animals from "fluid-like" to "elastic shelled"
76 organisms (Stanton et al., 1994, 1998a, 1998b). This approach has been used since the late
77 1970s to identify and quantify zooplanktonic scatterers (Greenlaw, 1977; Holliday and Pieper,
78 1980; Madureira et al., 1993a,b). Less has been done to characterize micronektonic organisms
79 from the open sea, where micronekton are diverse and include small pelagic fishes,
80 cephalopods, large crustaceans and gelatinous animals. A recent biomass estimate of mid-
81 water fish was based on the 38 kHz frequency alone (Irigoien et al., 2014). Furthermore, the
82 difference of mean volume backscattering strength between two frequencies (38 and 120 kHz)
83 was used to differentiate "fish", "macrozooplankton" and "zooplankton" scatterers (Fielding
84 et al., 2012; Bedford et al., 2015).

85 In the Southern Ocean (water masses south of the Subtropical Front), the importance
86 of micronekton is illustrated by the considerable populations of subantarctic seabirds and
87 pinnipeds that primarily prey on schooling myctophids, swarming euphausiids and hyperiid
88 amphipods (Cooper and Brown, 1990; Woehler and Green, 1992; Guinet et al., 1996; Bocher
89 et al., 2001). However, to our knowledge, acoustic investigation of mid-water organisms in
90 lower latitudes of the Southern Ocean is limited to a few surveys (Miller, 1982; Perissinotto
91 and McQuaid 1992; Pakhomov and Froneman, 1999), and only three recent studies
92 discriminated acoustic groups by their bi-frequency characteristics (Fielding et al., 2012;
93 Saunders et al., 2013; Bedford et al., 2015).

The main goal of the present work was to use bi-frequency acoustic data (38 and 120 kHz) combined with net sampling to calibrate an algorithm tool that discriminates groups of scatterers in an acoustically poorly-explored area. The targeted region was the productive oceanic zone off south-eastern Kerguelen Islands, because: (*i*) several significant populations of predators are known to feed on micronektonic organisms in the area during the summer months, namely Antarctic fur seals and king penguins on mesopelagic fishes (mainly myctophids) and macaroni penguins on euphausiids and hyperiids (Bost et al., 2002; Charrassin et al., 2004; Lea et al., 2002; C.A. Bost and Y. Cherel, unpublished data); and (*ii*) myctophid fishes and euphausiids were already successfully collected in the area (Duhamel et al., 2000, 2005; authors' unpublished data). The rationale was that different groups of micronektonic organisms (large crustaceans and mid-water fish) should be abundant in the targeted area and that the bi-frequency acoustic data should allow investigating their horizontal and vertical abundance patterns according to the type of structures (patches and layers).

2. Materials and methods

The oceanographic cruise (MD197/MYCTO) was carried out during the austral summer 2013-2014 on board the R/V *Marion Dufresne II*. The overall dataset was based on 1,320 km of acoustic data in oceanic waters off Kerguelen Islands during 14 consecutive days of recording.

2.1. Acoustic sampling

In situ acoustic data were recorded day and night during the period 23 January-5 February 2014. Measurements were made when cruising at a speed of 8 knots, using a Simrad EK60 split-beam echo sounder operating simultaneously at 38 and 120 kHz. The transducers were hull-mounted at a depth of 6 m below the water surface. An offset of 30 m below the surface was applied to account for: (*i*) the depth of the transducers, (*ii*) the acoustic Fresnel zone, and (*iii*) the acoustic interference from surface turbulence. Acoustic data were thus collected on a vertical range from 30 to 300 m according to the 120 kHz range (Fig. 1). The limited depth of 300m is considered in the interpretation of mid-water organisms distributions, especially for those which are known to perform vertical migration according to the day/night cycle (diel vertical migration; Lebourges-Dhaussy et al., 2000; Benoit-Bird et al., 2009) (*see section 4.2* below). Indeed, most of these organisms were sampled at night but only epipelagic and some mesopelagic organisms were observable during the day within this depth range.

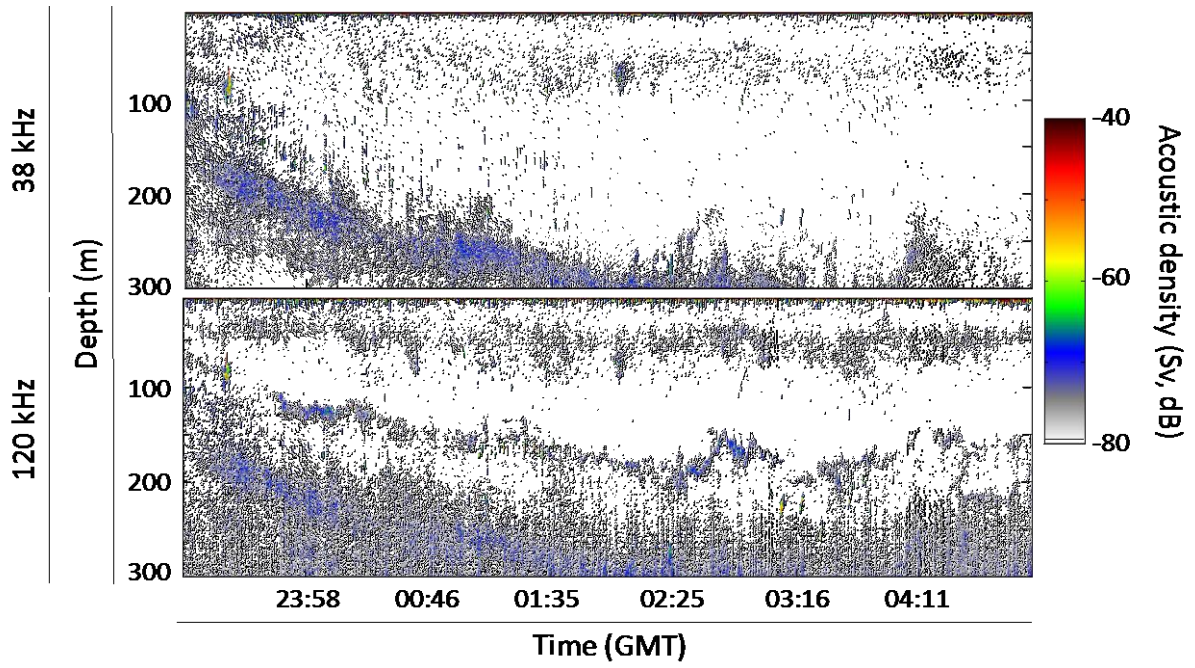

Fig. 1. 38 and 120 kHz echograms representing acoustic density (in color, S_v in dB) recorded on the 24th of January 2014 morning from 30 to 300m depth in east waters off Kerguelen.

Transducers were calibrated following the procedures recommended in Foote et al. (1987). Settings that were used during data acquisition are summarized in Table 1. Movies+ software (Ifremer development) was used for assessing visually the quality of the data prior further analyses. Depending on this quality assessment, data were filtered using an in-house tool (Béhagle et al., 2015) computed with Matlab (MATLAB 7.11.0.584, Release 2010b) and Movies3D software (Ifremer development) to remove ADCP (Acoustic Doppler Current Profiler) interference, background noise, and both attenuated- and elevated-signals. Then, an echo-integration by layer, with a threshold set at -80 dB to exclude scatterers which are not representative of micronektonic organisms, was applied on filtered acoustic data with an echo-integration cell size fixed at 3 pings per 1 m depth in order to smooth variability while keeping as much information as possible.

From echo-integration, volume backscattering strength (S_v, dB re 1 m^{-1}) was used to assess the mean echo level on both 38 and 120 kHz and thus to evaluate differences of relative frequency response of the organisms considered (*see section 2.3* below). Also, the acoustic

density of scatterers was estimated by calculating the Nautical Area Scattering Coefficient (NASC, s_A, $m^2 \cdot nmi^{-2}$; MacLennan et al., 2002). NASC was used as a proxy of relative biomass of acoustic targets, assuming that the composition of the scattering layers and the resulting scattering properties of biological organisms are homogeneous (*e.g.* Simmonds and MacLennan, 2005; Lawson et al., 2008).

Table 1. Simrad EK60 echo sounder parameter settings onboard the R/V *Marion Dufresne II* during the MD197/MYCTO cruise in January-February 2014.

	38 kHz	120 kHz
Max. power (W)	1000	250
Pulse duration (ms)	1.024	1.024
Ping interval (s)	1.5	1.5
Target Strength 'TS' gain (dB)	24.65	27.03
Area backscattering coefficient (Sa) correction	-0.75	-0.30
Sample length (m)	0.189	0.189

2.2. Biological sampling

To determine the species and size composition of the dominant scatterers, trawling of micronektonic animals was conducted using the Mesopelagos trawl that was designed by Ifremer (fisheries biology and technology laboratory, LTBH, Lorient, France) (Meillat, 2012). The non-closing trawl vertical and horizontal openings varied between 5 and 6 m and 10 and 12 m, respectively. The trawl has a mesh size of 4 cm in the wings, reducing to 5 mm at the codend during sampling. A terminal rigid collector was fixed on the codend in order to collect micronektonic organisms in good conditions. A Scanmar acoustic device (Åsgårdstrand, Norway) was attached on the net to monitor in real time the depth of trawling simultaneously to acoustic measurements (Williams and Koslow, 1997). The net was also equipped with an

elephant seal tag (Sea Mammal Research Unit, UK) that was fixed on the trawl headline. The tag was a multisensor data logger recording pressure (accuracy of 2 dbar) and hence depth, temperature, salinity and fluorescence (Blain et al., 2013). Only depth data were analyzed in the present work, thus providing an accurate time/depth profile for each tow. The trawl was towed for 30 min at targeted depth at a speed of 1.5-2.5 knots. All catches were sorted by species or lowest identifiable taxonomic groups, measured and weighed. While Antarctic krill (*Euphausia superba*) does not occur in the area, collected taxa were representative of the Polar Frontal Zone and Polar Front, including zooplankton-like organisms (*i.e.* euphausiids, amphipods, large copepods and non-gaseous gelatinous organisms), fish-like organisms (*i.e.* fish with a gas-filled swimbladder and gaseous gelatinous organisms), and other organisms (*i.e.* fish without a gas-filled swimbladder and small squids). Most of the 39 pelagic hauls conducted during this survey had mixed catches and were not further considered here. Indeed, to be able to calibrate as correctly as possible a bi-frequency algorithm in this area, we chose to use only mono-specific trawls. Two trawls were suitable for acoustic mark identification, because almost all the catches consisted of one single species in large quantity (*see section 2.3* below).

2.3. Bi-frequency method calibration

The acoustic properties of biological organisms vary with the operating frequency of the echo sounder. Therefore, comparing the echo levels of individual scatterers ensonified at different frequencies is likely to provide information on the types of targets that are present in the water column (Madureira et al., 1993a,b; Kang et al., 2002). According to the literature, zooplankton-like and non-gaseous gelatinous organisms have an increasing relative frequency response between 38 and 120 kHz (Stanton and Chu, 2000; David et al., 2001; Lavery et al., 2002; Korneliussen and Ona, 2003), whereas fish with a gas-filled swimbladder and gaseous

191 gelatinous organisms have a stable to decreasing relative frequency response between 38 and
192 120 kHz, depending on the size of the gaseous inclusion (Warren et al., 2001; Kloser et al.,
193 2002; Korneliussen and Ona, 2003) (Fig. 2). Thus, using the difference of reflectance of well-
194 characterized biological samples collected by trawls, we determined thresholds to obtain the
195 best compromise to separate three acoustic groups of organisms.
196

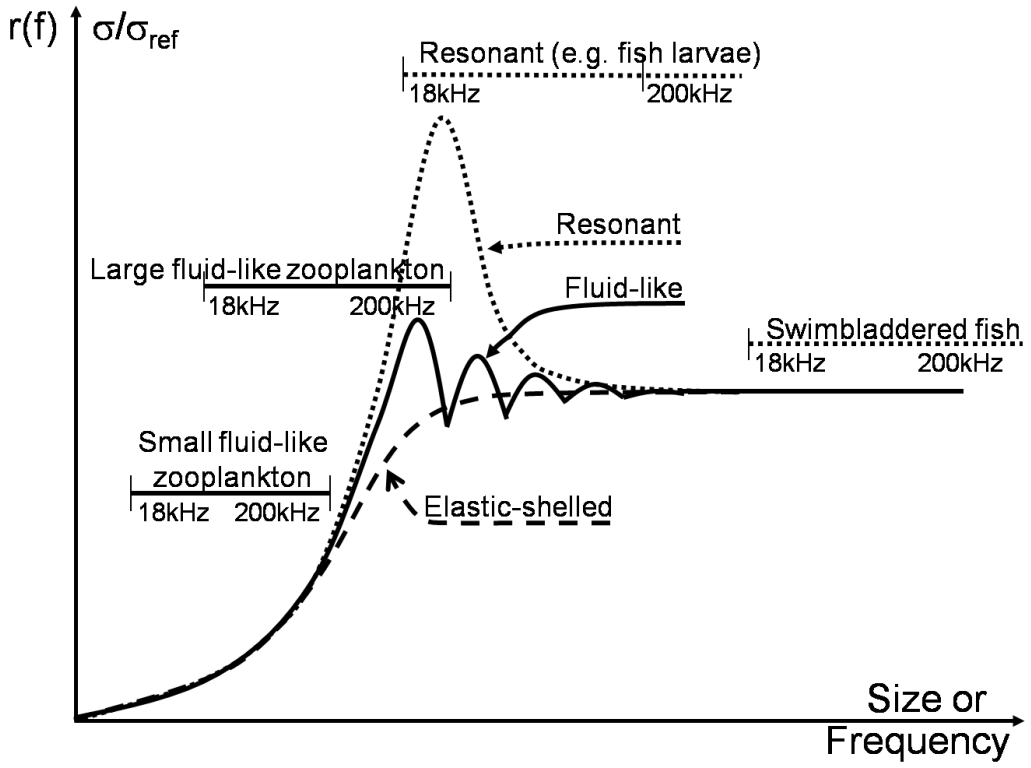

197

198 **Fig. 2.** Schematic description of the relative frequency response, r(f). Horizontal lines indicate
199 typical range positions of selected acoustic categories when measured at frequencies 18-200
200 kHz. Source: Korneliussen and Ona (2003).
201

202 Firstly, "fluid-like" organisms were discriminated from "gas-bearing" organisms
203 according to trawl sampling and to acoustic properties of scatterers at 120 and 38 kHz,
204 respectively (Simmonds and MacLennan, 2005). Thresholds used in the bi-frequency
205 algorithm to discriminate acoustic groups were fixed using acoustic data from two relevant

206 trawls, which were selected according to: (*i*) their depth (only trawls between the surface and
207 200 m depth were considered to minimize as much as possible interference from the saturated
208 outgoing signal at 120 kHz), and (*ii*) the quality of their acoustic data (mainly depending on
209 the weather; only trawls with more than 50% of clean pings were considered). Two night
210 trawls (T07, 50 m depth and T14, 70 m depth) were mono-specific in their composition,
211 containing almost exclusively adults of subantarctic krill *Euphausia vallentini* (15-24 mm
212 long) and juveniles of the demersal fish *Muraenolepis marmoratus* (31-40 mm long),
213 respectively. The latter corresponds to the pelagic stage of the species (Duhamel et al., 2005),
214 *i.e.* fish were 3-4 cm long and contained a well-developed gas-filled swimbladder, similar to
215 several species of myctophids (*Electrona carlsbergi*, *Krefftichthys anderssoni*,
216 *Protomyctophum* spp.; Saunders et al., 2013). The acoustic characteristics of samples from
217 these two trawl tows were considered as representative of "fluid-like" and "gas-bearing"
218 scatterers, respectively. Only the acoustic characteristics corresponding in time and depth to
219 the two trawls were taken into account to grade the bi-frequency algorithm in order to be sure
220 that they were related to the organisms effectively caught in the net. For doing this, we used
221 the time/depth data provided by the elephant seal tag for extracting the acoustic data from 2 m
222 above the headline up to 10 m below (or 2 m below the footrope) during a limited time period
223 that focused on the acoustically detected aggregations (Fig. 3). The acoustic response at 38
224 and 120 kHz, of each echo-integration cell belonging to the trawl's path, was represented
225 relative to the 38 kHz frequency (Fig. 4a) to assess the positive *vs.* negative slope of the
226 relative frequency response between discrete 38 and 120 kHz frequencies.
227

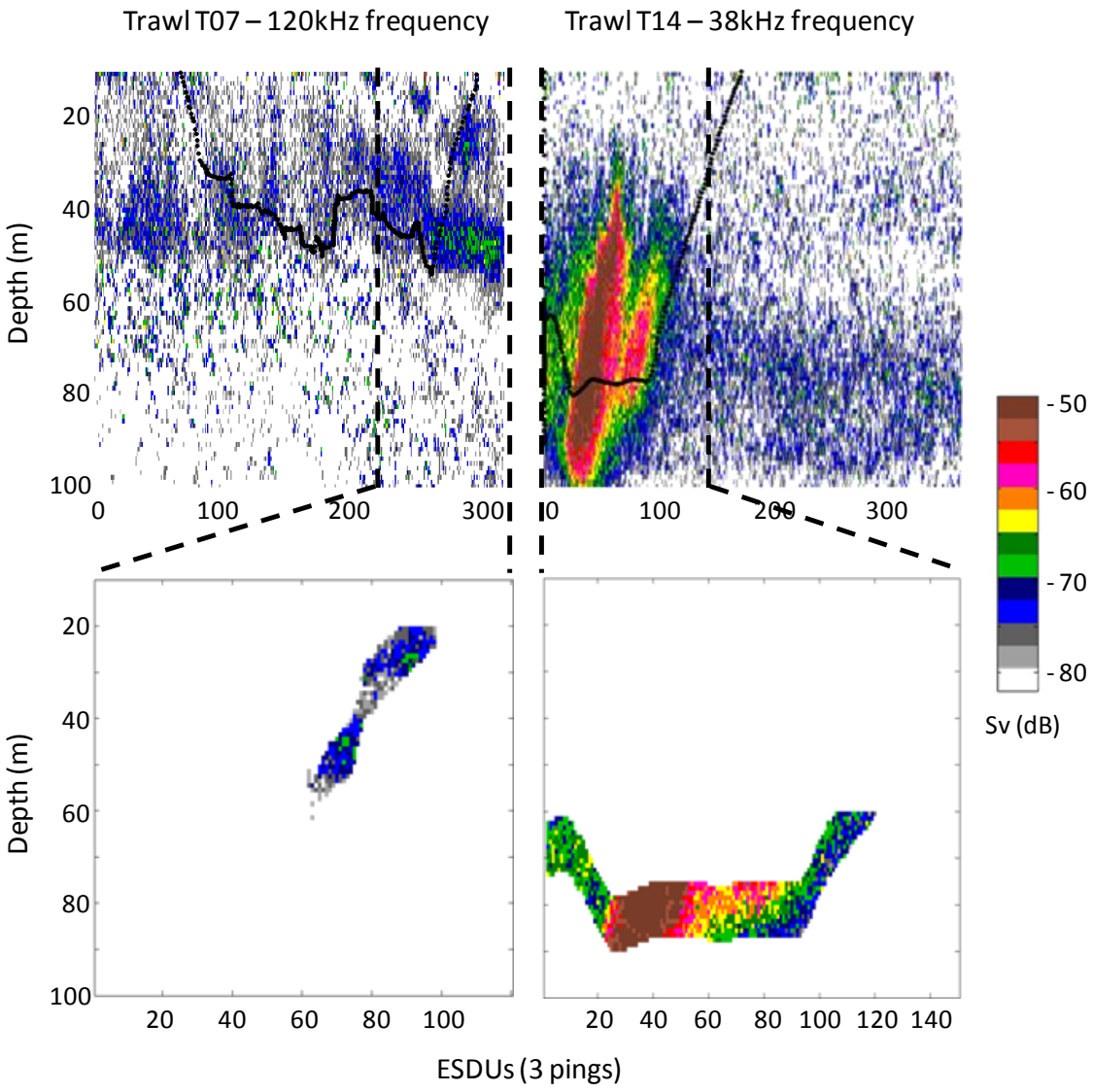

228

229 **Fig. 3.** Acoustic records and the corresponding cruise trawls (T07 and T14) that were used to
230 fix thresholds of difference in the bi-frequency algorithm. Upper panel: complete trawl
231 echograms with trawling depths (continuous black line) and limits of data extraction (dashed
232 black lines). Lower panel: extracted echogram samples focusing on the trawl targeted
233 aggregates that were selected from acoustic identification estimation. Left: T07 trawl
234 (euphausiids) sampling on the 120 kHz frequency to discriminate the "fluid-like" group.
235 Right: T14 trawl (gas-filled swimbladder fish) on the 38 kHz frequency to discriminate the
236 "gas-bearing" group.

Secondly, the difference in relative frequency response ($\Delta S_{v,120\text{-}38} = S_{v,120} - S_{v,38}$) was evaluated per echo-integration cell using a varying threshold of difference, ranging from -15 to 25 dB (Fig. 4b). For each threshold considered one by one, each acoustic sample was classified either in a group “lower than the threshold considered” or in the opposite group “higher than the threshold considered”. The total acoustic density was calculated (on 120 kHz samples for the “fluid-like” group and on 38 kHz samples for the “gas-bearing” group) for each of the lower/higher groups formed and reported in percentage to total acoustic density of the aggregate for each tested threshold (Fig. 4b).

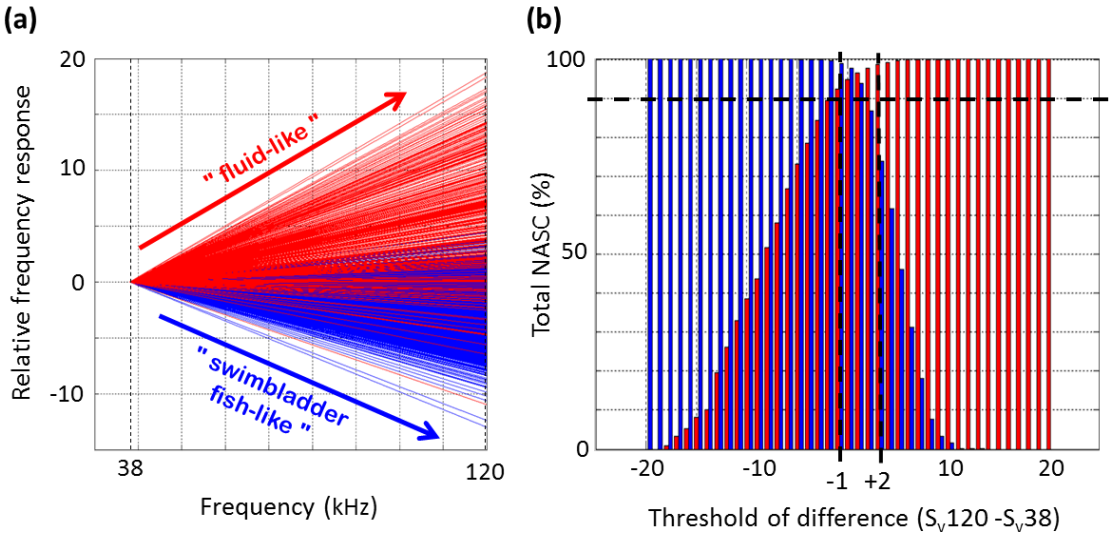

Fig. 4. Left panel (a): frequency response of each sample considered relatively to the 38 kHz frequency, with "fluid-like" samples (from the trawl T07) represented in red and "gas-bearing" samples (from the trawl T14) in blue. Right panel (b): bar chart of the percentage of "fluid-like" (in red) and "gas-bearing" (in blue) total NASC, according to a -15 to 25 dB range of threshold of difference, used to define the best thresholds (-1 and +2 dB) delimiting the “undetermined” group by transferring a maximum of 10% of their acoustic energy (total NASC).

Finally, the calculated "loss" of density for both "fluid-like" and "gas-bearing" groups was used to define two thresholds of differences delimiting the "undetermined" group by transferring a maximum of 10% of their acoustic energy (Fig. 4b) into the "undetermined" group. This group corresponds to an uncertainty zone where scatterers (*i*) have a close-to-flat relative frequency response between discrete 38 and 120 frequencies, (*ii*) cannot be allocated to "fluid-like" or "gas-bearing" organisms according to their S_v difference measured between 38 and 120 kHz but (*iii*) are potentially present in the water column and (*iv*) have no biological validation in this work. Preserving such a group allows accounting for organisms that could not be identified during this work from biological sampling but are present in the water column, while being more demanding on well-defined groups. Following this method, thresholds were defined at -1 and +2 dB. Scatterers with $\Delta S_{v,120\text{-}38}$ (*i*) > +2 dB are classified in the "fluid-like" group, (*ii*) < -1 dB are classified in the "gas-bearing" group and (*iii*) between -1 and +2 dB are classified in a third "undetermined" group (Fig. 5).

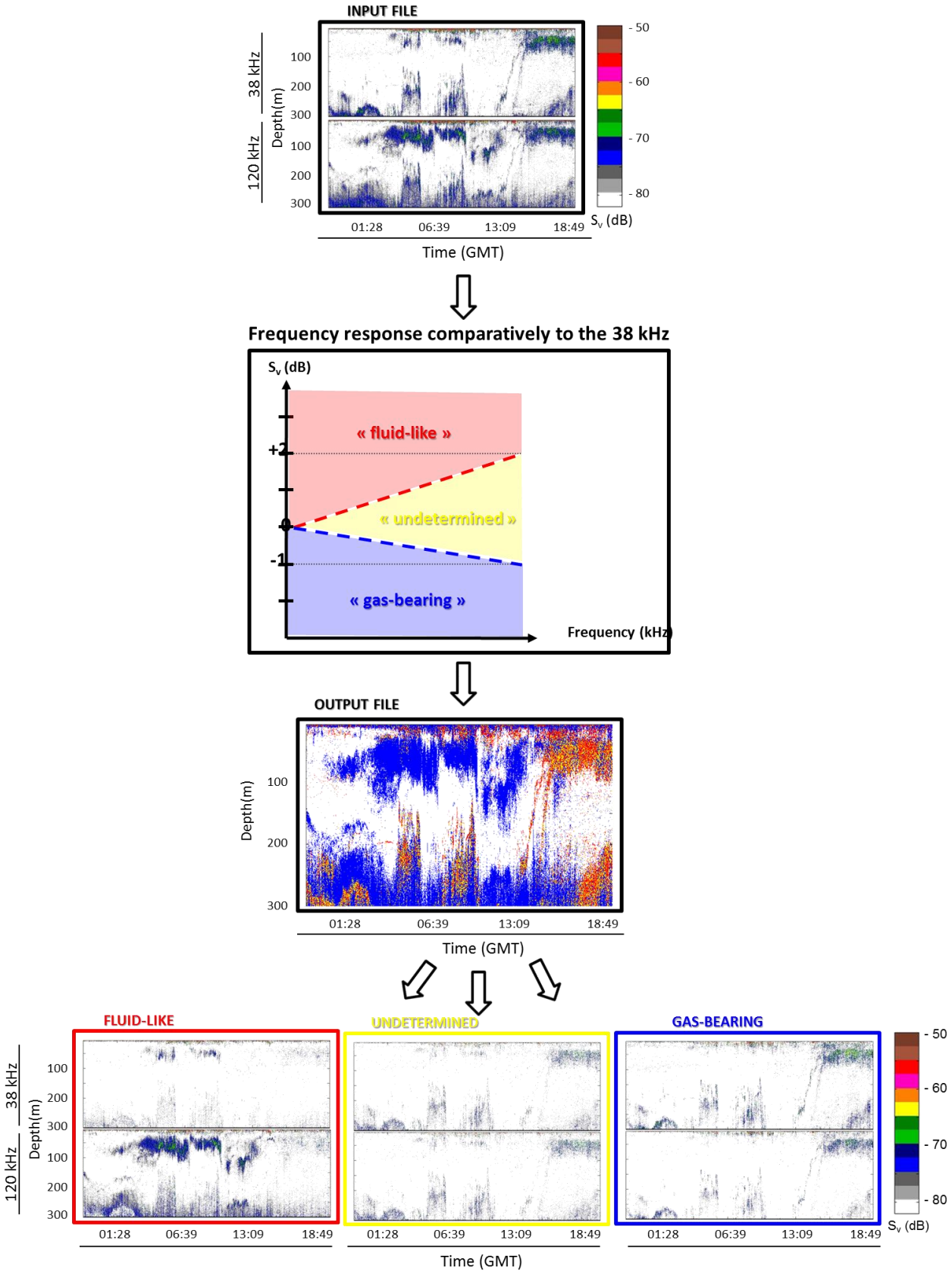

269

270 **Fig. 5.** Summary diagram of the bi-frequency algorithm method used in this study.

271 *2.4. Testing the bi-frequency algorithm*

272 The robustness of threshold values obtained by the bi-frequency algorithm developed
273 in the present work was tested by calculating the theoretical frequency responses of
274 *Muraenolepis marmoratus* and *Euphausia vallentini* using the mathematical models of Ye
275 (1997) and Stanton et al. (1994), respectively. While the Ye model provides an analytic
276 method for studying scattering of "gas-bearing" organisms at low frequencies, the Stanton
277 model focuses on the "fluid-like" organisms' acoustic properties.

278 The Ye (1997) model highlights a $\Delta S_{v,120\text{-}38}$ value of -0.4 dB for fish of 3 to 4 cm
279 length (as sampled during the T14 trawl), and the Stanton et al. (1994) model for randomly-
280 oriented fluid, bent cylinder highlights a $\Delta S_{v,120\text{-}38}$ value of +1.9 dB for euphausiids of 15-24
281 mm length (length range of organisms sampled during the T07 trawl). Using the bi-frequency
282 algorithm, the $\Delta S_{v,120\text{-}38}$ thresholds amounted to -1 and +2 dB, respectively, and are thus
283 consistent with the results of mathematical models. Our threshold values were even stronger
284 than those of the models ($-1 < -0.4$ and $2 > 1.9$ dB), thus highlighting the selectivity of the
285 algorithm. According to biological samples (see *section 2.2.* above) and acoustic properties of
286 scatterers at 38 and 120 kHz (see *section 2.3* above), three acoustic groups have been defined
287 for micronektonic organisms: (*i*) "gas-bearing" ($\Delta S_{v,120\text{-}38} < -1$ dB), (*ii*) "fluid-like" ($\Delta S_{v,120\text{-}38}$
288 > 2 dB), and (*iii*) "undetermined" scatterers ($-1 < \Delta S_{v,120\text{-}38} < 2$ dB).

289

290 *2.5. Data post-processing and statistical analyses*

291 Each echo-integration cell was attributed to "fluid-like", "undetermined" or "gas-
292 bearing" group based on its relative frequency response. Moreover, as living organisms
293 follow non-random and non-uniform distributions (Margalef, 1979; Legendre and Fortin,
294 2004), acoustic data were analyzed separately in terms of patches and layers.

First of all, in order to get homogenous horizontal sampling at high resolution, filtered data at 38 and 120 kHz have been echo integrated in cells of 10 m (horizontal) by 1 m (vertical). Patches were here defined as isolated groups of echo-integrated cells limited in space (between 10 and 3000 m long) and associated to a mean volume backscattering strength $S_v \geq$ -63 dB on the mean 38 and 120 kHz echogram. In contrast, layers were defined as continuous and homogenous areas of acoustic detections with a mean $S_v <$ -63 dB for each echo-integrated cell on the mean 38 and 120 kHz echogram. The -63 dB threshold was defined by the operator after a visual analysis of the number of patches detected along a representative acoustic sample of five hours long and along increasing S_v values from -70 to -40 dB. The value of -63 dB corresponds to a threshold level over which the number of patches did not further increased (Fig. 6).

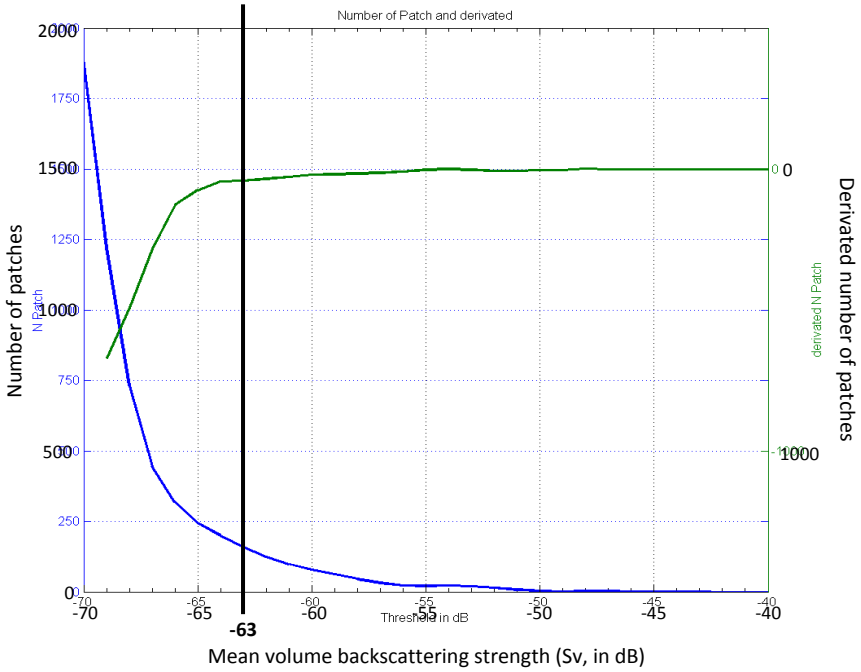

Fig. 6. Representative diagram of the number of patches (in blue) and its derivative (in green) detected along increasing S_v values from -70 to -40 dB. The value of -63 dB corresponds to a threshold level over which the number of patches did not further increased.

311 Using the Matlab contouring tool, echo-integrated cells having a mean $S_v \geq$ -63 dB
312 were extracted from the echo integrated datasets and each contour considered as a detected
313 patch (Fig. 7a). For each patch, mean depth, vertical size, mean S_v and mean NASC values at
314 both frequencies were computed. NASC values were first summed on the vertical and then
315 averaged on the horizontal. Cells that were not considered as patches were considered as
316 layers (Fig. 7b).

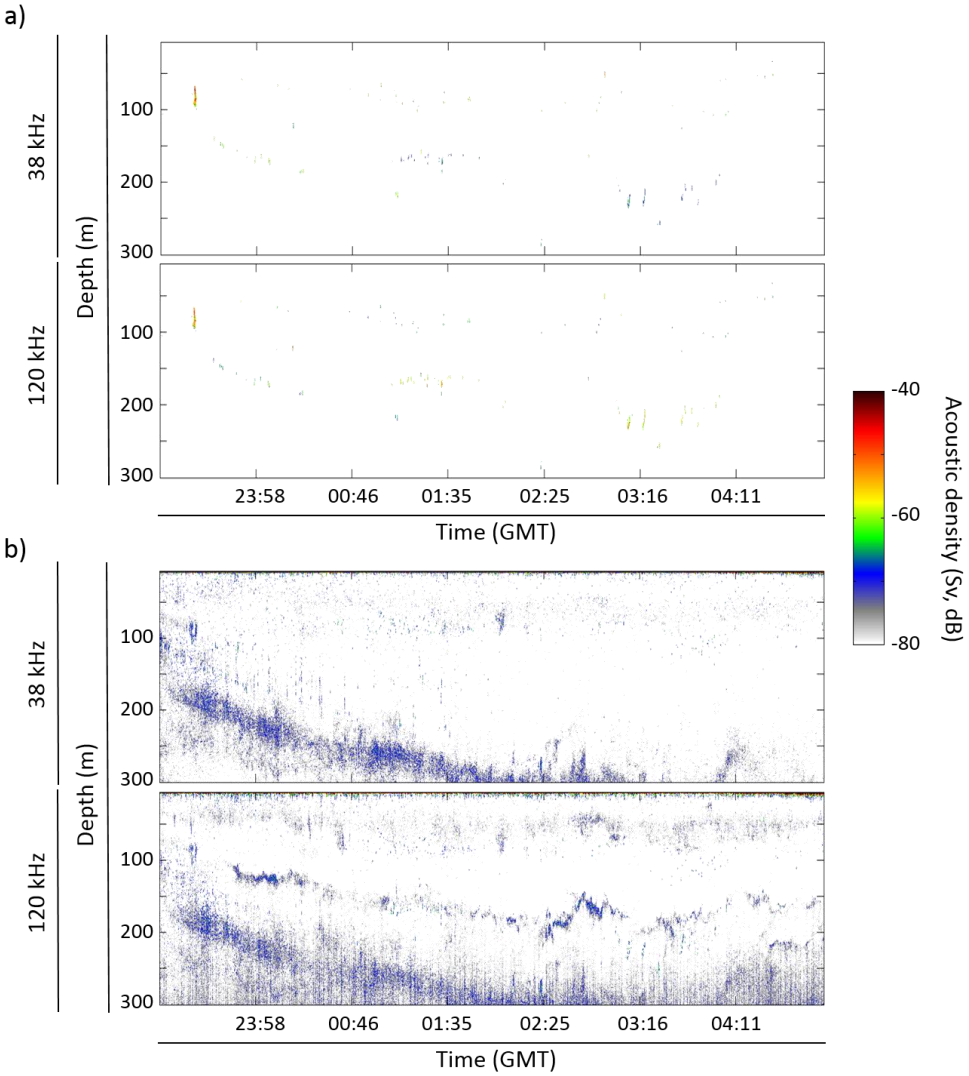

317

318 **Fig. 7.** 38 and 120 kHz echograms representing acoustic density (in color, S_v in dB) recorded
319 on the 24th of January 2014 morning from 30 to 300m depth in east waters off Kerguelen for
320 (a) patches- and (b) layers structures.

Total-, patches- and layers- datasets were then post-processed following the same bi-frequency algorithm (*see section 2.3* above). Thus, nine datasets were obtained: "fluid-like", "gas-bearing", and "undetermined" for layer structures, for patch structures, and for the whole (*i.e.* patches and layers together).

Acoustic data were analyzed from 30 to 300 m depth according to the applied offset (*see section 2.1.* above) and the 120 kHz emission range. Day and night data were analyzed separately because many mid-water organisms undergo diel vertical migration. The crepuscular period (45 minutes before and after sunrise and sunset) during which mid-water organisms ascend and descend (Lebourges-Dhaussy et al., 2000; Benoit-Bird et al., 2009) were excluded from the analyses.

Statistical analyses were performed within the R environment (R Core Team, 2014). Differences of distribution between groups were statistically assessed using student t tests.

3. Results

3.1. Horizontal distribution of acoustic groups of micronekton

The horizontal distribution of NASC values (on 38 kHz for "gas-bearing" and "undetermined" groups; on 120 kHz for "fluid-like" group) in the 30-300 m depth range varied spatially (Northern and Southern tracks), and according to the daily cycle (day and night), the type of structures (patches and layers) and the three acoustically-defined groups of micronektonic organisms (Fig. 8, Tables 2 and 3). Several features were notable: (*i*) total integrated NASC values were ~2-3 times higher in the Northern than in the Southern tracks; (*ii*) with one exception (see below), NASC values of each group were higher at night than during the day; (*iii*) a much larger proportion of scatterers of the three groups occurred in layers than in patches; (*iv*) the layers/patches difference was more pronounced at day than during the night, with patches almost disappearing at night (< 1% of the total NASC values); and (*v*) during the day, a higher NASC proportion of "gas-bearing" (10-26%) and "undetermined" (10-34%) than "fluid-like" (4-5%) scatterers occurred in patches.

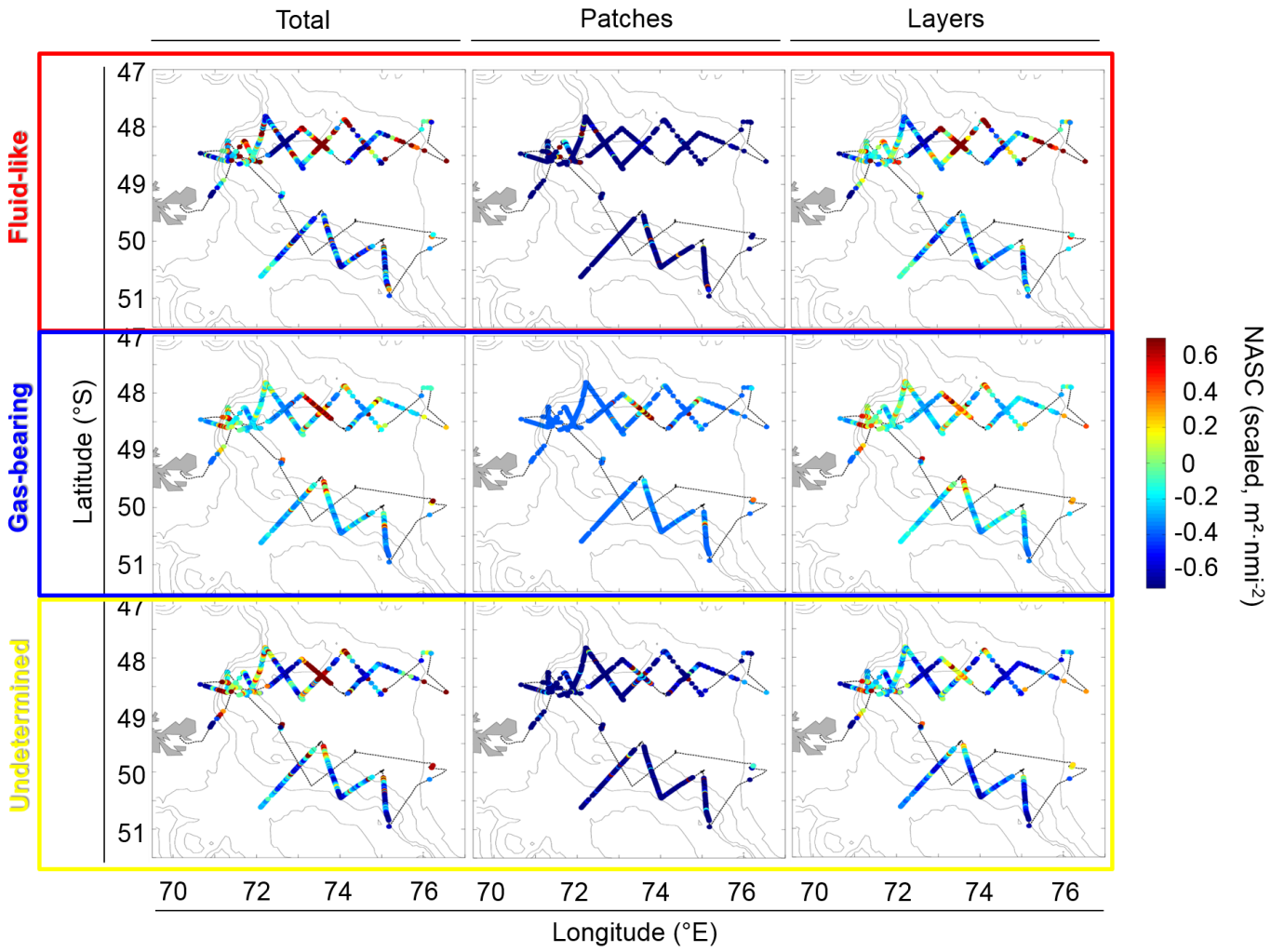

349

350 **Fig. 8.** Total density (NASC, scaled in $m^2 \cdot nmi^{-2}$, colored on ship track) observed during the cruise integrated from 30 to 300 m depth for each

351 acoustic group ("gas-bearing", fluid-like" and "undetermined" groups) and for each type of structure (patches and layers).

Table 2. Acoustic density (NASC, in $m^2 \cdot nmi^{-2}$) per echo-integration cell of each acoustic group ("gas-bearing", "fluid-like" and "undetermined" groups). Values are means ± SD. The small size of the 10 m horizontal cells explains both their numbers and very large variances.

Time period	Tracks	Echo-integration cell per 10 m (n)	Total NASC values at 38 or 120 Hz ($m^2 \cdot nm^{-2}$)	"Fluid-like" NASC values at 120 kHz ($m^2 \cdot nm^{-2}$)	"Gas-bearing" NASC values at 38 kHz ($m^2 \cdot nm^{-2}$)	"Undetermined" NASC values at 38 kHz ($m^2 \cdot nm^{-2}$)
Day	Northern	69150	446 ± 3402	283 ± 2641	107 ± 1073	56 ± 756
	Southern	37724	273 ± 1642	209 ± 1507	42 ± 563	22 ± 136
	Both tracks	106874	385 ± 2907	257 ± 2305	84 ± 372	44 ± 614
Night	Northern	15252	649 ± 3091	351 ± 2432	225 ± 1487	73 ± 454
	Southern	5065	195 ± 579	73 ± 431	84 ± 372	38 ± 32
	Both tracks	20317	536 ± 2701	282 ± 2122	190 ± 1303	64 ± 394
Day and night	Northern	84402	483 ± 3349	295 ± 2604	129 ± 1160	59 ± 711
	Southern	42789	264 ± 1555	193 ± 1423	47 ± 544	24 ± 128
	Both tracks	127191	409 ± 2875	261 ± 2277	101 ± 998	47 ± 584

Table 3. Acoustic density (NASC, in $m^2 \cdot nmi^{-2}$) summed in the 30-300 m depth range and percentage contributions (between brackets) of each acoustic group ("gas-bearing", "fluid-like" and "undetermined" groups) as patches and layers (see text for definitions). Daytime and nighttime were considered separately, as the Northern and Southern tracks were.

Tracks	Groups	Day			Night		
		Total (10^6 m^2 nmi^{-2})	Patches (%)	Layers (%)	Total (10^6 m^2 nmi^{-2})	Patches (%)	Layers (%)
Northern	Gas-bearing	11.68 (25.9)	10.3	89.7	5.64 (32.0)	0.8	99.2
	Fluid-like	29.30 (65.0)	4.7	95.3	10.41 (59.1)	0.8	99.2
	Undetermined	4.10 (9.1)	9.7	90.3	1.56 (8.9)	0.7	99.3
	Total	45.08 (100.0)	6.6	93.4	17.61 (100.0)	0.8	99.2
Southern	Gas-bearing	2.23 (12.9)	26.1	73.9	0.68 (44.4)	0.5	99.5
	Fluid-like	14.21 (82.2)	3.4	96.6	0.66 (43.2)	0.0	100.0
	Undetermined	0.85 (4.9)	34.0	66.0	0.19 (12.5)	0.2	99.8
	Total	17.30 (100.0)	7.9	92.1	1.53 (100.0)	0.2	99.8
Total	Gas-bearing	13.92 (22.3)	12.8	87.2	6.31 (33.0)	0.8	99.2
	Fluid-like	43.51 (69.8)	4.3	95.7	11.07 (57.8)	0.8	99.2
	Undetermined	4.95 (7.9)	13.9	86.1	1.75 (9.2)	0.6	99.4
	Total	62.38 (100.0)	6.9	93.1	19.14 (100.0)	0.8	99.2

366 *3.2. Vertical distribution of acoustic groups of micronekton*

367

368 The vertical distribution of NASC values of the three acoustically-defined groups of
369 micronektonic organisms varied spatially (Northern and Southern tracks), temporally (time of
370 the day), and according to the type of structures (patches and layers) (Fig. 9, Table 4).
371 Overall, "fluid-like" organisms were structured in layers and their NASC values showed: (*i*) a
372 peak at shallow depths (< 100 m) during the day with an intermediate inter-quartile range
373 revealing a rather unimodal vertical distribution; and (*ii*) a progressive increase with depth
374 from 150 to 300 m. The pattern was similar at night, but with significantly lower values ($t = 17.5$, $p < 0.001$) and higher inter-quartile range, highlighting a consistent distribution in the
375
376 range 30-300 m. "Gas-bearing" scatterers showed a different vertical pattern with a well-
377 defined change between day and night. While most scatterers were structured in layers, they
378 were more patchily distributed during the day with a main mode at ~150 and ~70 m in the
379 Northern and Southern tracks, respectively. Patches almost completely disappeared at night
380 during which "gas-bearing" organisms occurred in more diffuse layers with a unimodal
381 distribution in the north at ~30 m and a bimodal distribution in the south at ~65 and ~200 m.
382 The distribution of "undetermined" organisms showed no obvious patterns, with discrete
383 small patches during the day and more obvious layers at night, especially at shallow depths in
384 the Northern track (Fig. 9, Table 4).

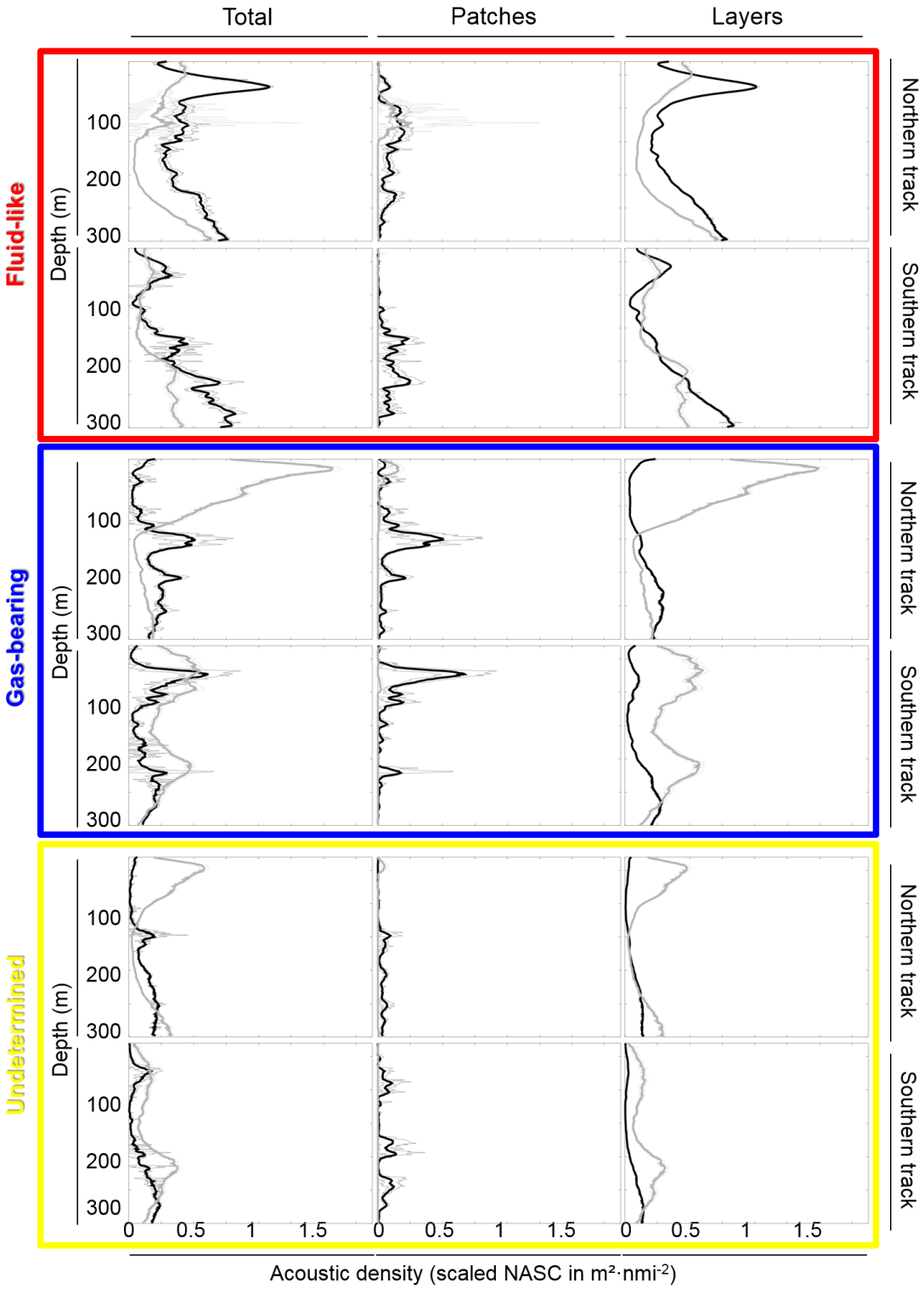

385

386 **Fig. 9.** Mean vertical NASC profiles from 30 to 300 m depth of each acoustic group ("gas-
387 bearing", fluid-like" and "undetermined" groups) for day (black lines) and night (grey lines)
388 and for each type of structures (patches and layers). Dashed lines indicate the 95% confidence
389 intervals.

Table 4. Maximum acoustic density (NASC) depth, median acoustic density and inter-quantile range proportion of acoustic groups (calculated on the 38 kHz for the "gas-bearing" and "undetermined" groups and on the 120 kHz for the "fluid-like" group) according to the tracks (Northern and Southern), time of the day (day and night) and type of structures (patches and layers).

Timing	Tracks	Groups	Maximum NASC depth (m)	Median NASC values (m^2 nmi^{-2})	Inter-quantile range (%)
Total					
Day	Northern	Gas-bearing	148	0.16	24.6
		Fluid-like	66	0.36	23.9
		Undetermined	147	0.09	50.0
	Southern	Gas-bearing	72	0.11	19.3
		Fluid-like	275	0.23	47.7
		Undetermined	270	0.05	54.5
Night	Northern	Gas-bearing	42	0.13	27.3
		Fluid-like	295	0.20	50.0
		Undetermined	45	0.10	33.3
	Southern	Gas-bearing	65	0.23	34.7
		Fluid-like	294	0.13	54.3
		Undetermined	214	0.12	25.0
Patches					
Day	Northern	Gas-bearing	147	0.03	10.4
		Fluid-like	109	0.05	17.1
		Undetermined	143	0.02	30.0
	Southern	Gas-bearing	68	0.01	9.7
		Fluid-like	163	0.02	36.4
		Undetermined	194	0.01	27.8
Night	Northern	Gas-bearing	45	0.00	7.1
		Fluid-like	122	0.00	0.0
		Undetermined	41	0.00	0.0
	Southern	Gas-bearing	94	0.00	0.0
		Fluid-like	38	0.00	0.0
		Undetermined	58	0.00	0.0
Layers					
Day	Northern	Gas-bearing	230	0.13	59.3
		Fluid-like	65	0.31	32.9
		Undetermined	297	0.04	53.8
	Southern	Gas-bearing	263	0.07	54.2
		Fluid-like	292	0.21	39.7
		Undetermined	297	0.02	46.2
Night	Northern	Gas-bearing	42	0.14	27.7
		Fluid-like	294	0.22	45.3
		Undetermined	45	0.09	36.6
	Southern	Gas-bearing	65	0.28	33.3
		Fluid-like	294	0.19	53.7
		Undetermined	214	0.10	27.6

4. Discussion

Historically, most of the acoustic investigations conducted in the Southern Ocean since the 1960s focused on Antarctic krill (Demer and Conti, 2005; Fielding et al., 2014), due to its high and variable biomass (Atkinson et al., 2009), key role in the high-latitude pelagic ecosystem (Ainley and DeMaster, 1990) and developing commercial fisheries (Nicol et al., 2012). More recently, the concept of a distinct Antarctic open-ocean food chain where Antarctic krill is absent pointed out the importance of other micronektonic organisms, including mid-water fish (Rodhouse and White, 1995). Hence, different groups were acoustically characterized in the Antarctic krill zone (Fielding et al., 2012; Saunders et al., 2013), but, to our knowledge, little acoustic information is available in Northern waters of the Southern Ocean where Antarctic krill is ecologically replaced by other micronektonic organisms, namely euphausiids, a few hyperiid amphipods and myctophid fishes.

The present study focused on productive waters off eastern Kerguelen Islands, where numerous top predators target micronektonic organisms different from Antarctic krill (Guinet et al. 1996). It provides a first depiction of horizontal and vertical (30-300 m) distribution and abundance of three different acoustic groups of micronektonic organisms from a bi-frequency processing of acoustic data (38 and 120 kHz).

4.1. Methodological comments and biological interpretation of the acoustic groups

Methodologically, the frequency-dependent technique based on estimated differences between mean volume-backscattering strength at 38 and 120 kHz has also previously been used to characterize acoustic groups (Madureira 1993a,b; Brierley et al., 1998). The most recent investigations defined two micronektonic groups in Antarctic waters, namely Antarctic

krill (macrozooplankton) that was identified using a 2-12 or 2-16 dB $\Delta S_{v,120-38}$ window (Fielding et al., 2012, 2014), and myctophids (gas-filled swimbladder fish) that were characterized by $\Delta S_{v,120-38} < 2$ or < 0 dB (Fielding et al., 2012; Saunders et al. 2013). Elsewhere, a threshold at $\Delta S_{v,120-38} = 2$ dB was used to discriminate gas-filled swimbladder fish (< 2 dB) from euphausiids (> 2 dB) (De Robertis et al., 2010; Ressler et al., 2015). Using the same overall approach, our $\Delta S_{v,120-38}$ threshold values fit well with theoretical models (Ye, 1997; Stanton et al., 1994). The $\Delta S_{v,120-38}$ threshold value (-1 dB) to discriminate "gas-bearing" backscatters was even lower than the previously used values (0-2 dB). Hence, our identification of "gas-bearing" backscatters is more conservative than in previous investigations, and the method allowed discriminating a third intermediate group of backscatters at $-1 < \Delta S_{v,120-38} < 2$ dB that cannot be classified as a given type of organism without ground-truthing.

Micronektonic organisms that constituted the three acoustic groups of backcatters can be tentatively defined using a combination of bi-frequency threshold values, acoustic sampling depth (30-300 m), net sampling (Hunt et al., 2011) and predators' diet (Guinet et al., 1996) within the studied area. (*i*) The "fluid-like" group ($\Delta S_{v,120-38} > 2$ dB) is likely to correspond primarily to crustaceans, including euphausiids (*e.g. Euphausia vallentini, E. triacantha, Thysanoessa* spp.) and hyperiids (*Themisto gaudichaudii*). Non-gas-bearing gelatinous organisms (*e.g.* salps) also occur in the area (Hunt et al., 2011) and they were collected during the cruise, it is here assumed that their acoustic signature was similar to "fluid-like" signature (Wiebe et al., 2010). (*ii*) The "gas-bearing" group ($\Delta S_{v,120-38} < -1$ dB) includes gas-bearing gelatinous organisms and gas-filled swimbladder fish. Siphonophores occur in the Southern Ocean, but their abundance is relatively low in Kerguelen waters (Hunt et al., 2011). On the other hand, mesopelagic fish were abundant, with most of them belonging to the Family Myctophidae in terms of species, number and biomass (Duhamel et

al., 2005). Not all myctophid species contain a gas-filled swimbladder, however, and it is likely that the acoustically detected myctophids were primarily *Electrona carlsbergi*, *Krefftichthys anderssoni* and *Protomyctophum* spp. although it was not possible to differentiate between species (Marshall, 1960; Saunders et al., 2013). Noticeably, all those species are targeted by the myctophid-eater king penguin (Bost et al., 2002; Cherel et al., 2002) and they are known to form school structures (Saunders et al., 2013). *Krefftichthys anderssoni* was the commonest net-caught myctophid during the cruise and *Protomyctophum bolini* and *P. tenisoni* also occurred in significant numbers in trawls (authors' unpublished data). (*iii*) The "undetermined" group of scatterers ($-1 < \Delta S_{v,120\text{-}38} < 2$ dB) most likely corresponds to other fish, meaning lipid-filled swimbladder species and fish with no swimbladder (Simmonds and MacLennan, 2005). Again these characteristics point out myctophid fish in the area, including *Gymnoscopelus braueri* that ranked third amongst the net-caught myctophids during the cruise (authors' unpublished data) together with other *Gymnoscopelus* species that constitute the main prey species of fur seals *Arctocephalus* spp. (Marshall, 1960; Lea et al., 2002; Saunders et al., 2013). Theoretically also, the "undetermined" group can include a combination of "fluid-like" and "gas-bearing" scatterers living in mixed and homogenous layers or patches, thus overall resulting in intermediate $\Delta S_{v,120\text{-}38}$ values.

4.2. Horizontal and vertical distribution of the acoustic groups

The acoustic density (NASC) of micronektonic scatterers varied both in time and space, thus showing a complex pattern depending on acoustically-defined groups, time of the day (day/night), depth (30-300 m), the type of structures (patches and layers) and geography (Northern and Southern tracks). Firstly, depth-integrated NASC values of the three acoustic

groups were higher in the Northern than the Southern tracks, which may correspond to the Polar Front and Northern Antarctic waters, respectively. This would be consistent with the high abundance of micronekton recorded in frontal areas of the Western Indian sector of the Southern Ocean (Pakhomov et al., 1996; Pakhomov and Froneman, 2000) and deserves a thorough study in combination with hydrographic data. Secondly, the finding of an overall higher biomass at night than during the day is in accordance with a recent large-scale acoustic investigation in the Western Indian Ocean (Béhagle et al. 2015) and the general trend of upward migration of deep-dwelling zooplanktonic and micronektonic organisms at sunset in oceanic waters (Domokos, 2009; Escobar-Flores et al., 2013; Béhagle et al., 2014). Finally, other key features of micronektonic distribution were the much higher NASC values in layers (> 92% of total NASC values) than in patches, and the almost disappearance of patches (< 1%) at night when compared to the daylight hours (Table 4). The latter feature is related to the diel behaviour of mid-water organisms that disperse at night to feed in the epipelagic zone (Hays, 2003). Moreover, in this work, the potential bias in patches detection linked to the increasing acoustic beam with depth is not considered as well as the depth is not a hindrance to our comparisons. Indeed, (*i*) in most cases, the absence of patches at night makes the comparison between day and night NASC proportions meaningful and independent of depth and (*ii*) for the only case of night occurrence of patches (along the Northern track for "fluid-like" organisms), the few detected patches were observed at the same depth as during the day which makes comparison possible regardless of any difference in resolution of detecting patches. The only bias could be an underestimation of deep patches detected during the day.

"Fluid-like" scatterers occurred predominantly within layers with a bimodal distribution at shallow and deep depths (Fig. 9). A similar bimodal vertical distribution was previously observed from acoustic-based records at the Polar Front area westward (Pakhomov

et al., 1994). A prominent feature of "fluid-like" scatter occurrence in Kerguelen waters was a well-defined layer at ~60 m depth during the day, which likely corresponds to some key crustacean species collected with nets (*E. vallentini*, *Thysanoessa* spp., *T. gaudichaudii*; Pakhomov and Froneman, 1999; Hunt et al., 2011; this study). Noticeably, those crustacean species form the bulk of the food of the most abundant diving air-breathing predator from the area, the macaroni penguin (*Eudyptes chrysolophus*), which predominantly forages at 20-60 m depth during the day (Sato et al., 2004; Bost and Cherel, unpublished data).

Most scatterers of the "gas-bearing" and "undetermined" groups were structured in layers that were more pronounced at night than during the day. Especially obvious was a ~50 m-deep layer during the northern track that suggests a high abundance of mid-water fish in the upper epipelagic at night. Indeed, surface layers are invaded at that time by myctophids in Kerguelen waters and elsewhere, with the species including a pool of gas-filled swimbladder-, lipid-filled swimbladder- and swimbladderless myctophids (Duhamel et al., 2005; Collins et al., 2012; Saunders et al., 2013). This pattern corresponds well with the night-time diving behaviour of Antarctic fur seals (*A. gazella*) that prey primarily on mid-water fish at 40-60 m depth in eastern Kerguelen waters (Lea et al., 2002, 2006). A major characteristic of the "gas-bearing" group was the significant amount of scatterers structured in patches during daytime. It is likely that patches corresponded to schools of fish, as already depicted in the Atlantic sector of the Southern Ocean (Fielding et al., 2012; Saunders et al., 2013), and that the species were mainly myctophids with a gas-filled swimbladder (Collins et al. 2008). Patch depth observed during the survey was < 180 m, thus suggesting that they were composed of *Krefftichthys anderssoni* and *Protomyctophum* spp., and not of deeper-living species as *E. carlsbergi* (Duhamel et al., 2005; Collins et al., 2008; Flynn and Williams, 2012). Indeed, the survey overlapped the foraging area of the king penguin (*Aptenodytes patagonicus*) that is known to target primarily *K. anderssoni* in the 100-150 m depth range during the day (Bost et

al., 2002; Charrassin et al., 2004; C.A. Bost and Y. Cherel, unpublished data). Interestingly, patches occurred at different depths during the northern (~150 m) and southern (~70 m) tracks, which can be related to different species within patches or to physical oceanography in different water masses or to a combination of both. The limited information available shows that myctophids are linked to the physical, chemical and biological characteristics of the water column, with bottom depth, temperature and oxygen content of the water being key environmental factors controlling their distributions (Hulley and Lutjeharms, 1995). Moreover, despite patches were detected only during daylight, variations in light levels could also affect the vertical distribution of mesopelagic organisms as it has been observed for deep scattering layers (Klevjer et al., 2016).

In conclusion, the present study highlights the usefulness of combining acoustic records with biological sampling to use reliable bi-frequency algorithms to discriminate groups of backscatters. When validated, the method bypasses the problem of net avoidance by micronekton, especially during the daylight hours (Kloser et al., 2009; Pakhomov and Yamamura, 2010; Kaartvedt et al., 2012). Despite uncertainties with species identification and depth limitation in acoustic data, it provides an essential descriptive baseline of the spatial distribution and structure of micronektonic organisms. More at-sea investigations are needed to better define the species-specific acoustic response of crustaceans (*e.g.* Madureira et al., 1993b), myctophids (*e.g.* Gautier et al., 2014) and gelatinous organisms (*e.g.* Wiebe et al., 2010). As it stands, however, the method can already help (*i*) to link micronektonic group distribution to physical oceanography both horizontally and vertically to better define their oceanic habitats (Koubbi et al., 2011), (*ii*) to investigate predator-prey interactions by combining real time acoustic surveys and bio-logging (Benoit-Bird et al., 2011; Bedford et al., 2015), and hence (*iii*) to gather useful information on the functioning of the still poorly known oceanic ecosystem. Overall, the distribution of the acoustic groups fit well with the at-

sea behaviour of air-breathing diving predators from Kerguelen Islands (see above). More specifically, however, a thorough comparison between net trawling and predator foraging ecology underlines some fundamental mismatches that can be investigated using active acoustic surveys. For example, the subantarctic krill *E. vallentini* is traditionally considered to live deeper than 100 m during the day (Perissinotto and MacQuaid, 1992; Hamame and Antezana, 2010), while it is one of the most important prey items of various diurnal seabirds (*e.g.* crested penguins) that feed primarily in the top 50 m of the water column (Ridoux, 1988; Tremblay and Cherel, 2003; Sato et al., 2004).

Acknowledgements

The authors thank the officers, crew and scientists of the R/V *Marion Dufresne II* for their assistance during the research cruise LOGIPEV197. This work was supported financially and logistically by the Agence Nationale de La Recherche (ANR MyctO-3D-MAP, Programme Blanc SVSE 7 2011, Y. Cherel), the Institut Polaire Français Paul Emile Victor, and the Terres Australes et Antarctiques Françaises.

References

Ainley, D.G., DeMaster, D.P., 1990. The upper trophic levels in polar marine ecosystems in: Smith, W.O. (Ed.), Polar Oceanography, Part B. Academic Press, San Diego, pp. 599-630.

Atkinson, A., Siegel, V., Pakhomov, E.A., Jessopp, M.J., Loeb, V., 2009. A re-appraisial of the total biomass and annual production of Antarctic krill. Deep-Sea Res. I 56, 727-740.

Bedford, M. Melbourne-Thomas, J., Corney, S., Jarvis, T., Kelly, N., Constable, A., 2015. Prey-field use by a Southern Ocean top predator: enhanced understanding using integrated datasets. Mar. Ecol. Prog. Ser. 526, 169–181.

Béhagle, N., du Buisson, L., Josse, E., Lebourges-Dhaussy, A., Roudaut, G., Ménard, F., 2014. Mesoscale features and micronekton in the Mozambique Channel: an acoustic approach. Deep-Sea Res. II 100, 164-173.

574 Béhagle, N., Cotté, C., Ryan, T., Gauthier, O., Roudaut, G., Brehmer, P., Josse, E., Cherel, Y., 2016. Acoustic
575 micronektonic distribution structured by macroscale oceanography across 20-50°S latitudes in the
576 southwestern Indian Ocean. Deep-Sea Res. I 110, 20-32.
577 Benoit-Bird, K.J., Au, W.W.L., Wisdom, D.W., 2009. Nocturnal light and lunar cycle effects on diel migration
578 of micronekton. Limnol. Oceanogr. 54, 1789-1800.
579 Benoit-Bird, K.J., Kuletz, K., Heppell, S., Jones, N., Hoover, B., 2011. Active acoustic examination on the
580 diving behavior of murres foraging on patchy prey. Mar. Ecol. Prog. Ser. 443, 217-235.
581 Bertrand, A., Grados, D., Habasque, J., Fablet, R., Ballon, M., Castillo, R., Gutierrez, M., Chaigneau, A.,
582 Gutierrez, M., Josse, E., Roudaut, G., Lebourges-Dhaussy, A., Brehmer, P., 2013. Routine acoustic data
583 as new tools for a 3D vision of the abiotic and biotic components of marine ecosystem and their
584 interactions. Acoustics in Underwater Geosciences Symposium (RIO Acoustics), 2013 IEEE/OES,
585 DOI: 10.1109/RIOAcoustics.2013.6683995
586 Bianchi, D., Stock, C., Galbraith, E.D., Sarmiento, J.L., 2013. Diel vertical migration: ecological controls and
587 impacts on the biological pump in a one-dimensional ocean model. Global Biogeochem. Cycles 27,
588 478-491.
589 Blain, S., Renaud, S., Xing, X., Claustre, H., Guinet, C., 2013. Instrumented elephant seals reveal the seasonality
590 in chlorophyll and light-mixing regime in the iron-fertilized Southern Ocean. Geophys. Res. Lett. 40,
591 6368-6372.
592 Bocher, P., Cherel, Y., Labat, J.P., Mayzaud, P., Razouls, S., Jouventin, P., 2001. Amphipod-based food web:
593 *Themisto gaudichaudii* caught in nets and by seabirds in Kerguelen waters, southern Indian Ocean. Mar.
594 Ecol. Prog. Ser. 223, 261-276.
595 Bost, C., Zorn, T., Le Maho, Y., Duhamel, G., 2002. Feeding of diving predators and diel vertical migration of
596 prey: King penguin's diet versus trawl sampling at Kerguelen Islands Mar. Ecol. Prog. Ser. 227, 51-61.
597 Brierley, A.S., Ward, P., Watkins, J.L., Goss, C., 1998. Acoustic discrimination of Southern Ocean zooplankton.
598 Deep-Sea Res. II 45, 1155–1173.
599 Charrassin, J.B., Park, Y.H., Le Maho, Y., Bost, C.A., 2004. Fine resolution 3D temperature fields off Kerguelen
600 from instrumented penguins. Deep-Sea Res. I 51, 2091-2103.
601 Cherel, Y., Pütz, K., Hobson, K.A., 2002. Summer diet of king penguins (*Aptenodytes patagonicus*) at the
602 Falkland Islands, southern Atlantic Ocean. Polar Biol. 25, 898-906.
603 Collins, M.A., Xavier, J.C., Johnston, N.M., North, A.W., Enderlein, P., Tarling, G.A., Waluda, C.M., Hawker,
604 E.J., Cunningham, N.J., 2008. Patterns in the distribution of myctophid fish in the northern Scotia Sea
605 ecosystem. Polar Biol. 31, 837-851.
606 Collins, M.A., Stowasser, G., Fielding, S., Shreeve, R., Xavier, J.C., Venables, H.J., Enderlein, P., Cherel, Y.,
607 Van de Putte, A., 2012. Latitudinal and bathymetric patterns in the distribution and abundance of
608 mesopelagic fish in the Scotia Sea. Deep-Sea Res. II 59–60, 189–198.
609 Cooper, J, Brown, C.R., 1990. Ornithological research at the sub-Antarctic Prince Edward Islands: a review of
610 achievements. S. Afr. J. Antarct. Res. 20, 40-57.
611 David, P., Guérin-Ancey, O., Oudot, G., Van Cuyck, J.P., 2001. Acoustic backscattering from salp and target
612 strength estimation. Oceanol. Acta 24, 443-451.

Demer, D.A., Conti, S.G., 2005. New target-strength model indicates more krill in the Southern Ocean. ICES J. Mar. Sci. 62, 25–32.

De Robertis, A., McKelvey, D.R., Ressler, P.H., 2010. Development and application of an empirical multifrequency method for backscatter classification. Can. J. Fish. Aquat. Sci. 67, 1459–1474.

Domokos, R., 2009. Environmental effects on forage and longline fishery performance for albacore (*Thunnus alalunga*) in the American Samoa Exclusive Economic Zone. Fish. Oceanogr. 18, 419-438.

Duhamel, G,, Koubbi, P., Ravier, C., 2000. Day and night mesopelagic fish assemblages off the Kerguelen Islands (Southern Ocean). Polar Biol. 23, 106-112.

Duhamel, G., Gasco, N., Davaine, P., 2005. Poissons des îles Kerguelen et Crozet. Guide régional de l'océan Austral. Muséum national d'Histoire naturelle, Paris, France.

Escobar-Flores, P., O'Driscoll, R.L., Montgomery, J.C., 2013. Acoustic characterization of pelagic fish distribution across the South Pacific Ocean. Mar. Ecol. Prog. Ser. 490, 169-183.

Fielding, S., Watkins, J.L., Collins, M.A., Enderlein, P., Venables, H.J., 2012. Acoustic determination of the distribution of fish and krill across the Scotia Sea in spring 2006, summer 2008 and autumn 2009. Deep-Sea Res II 59, 173-188.

Fielding, S., Watkins, J.L., Trathan, P.N., Enderlein, P., Waluda, C.M., Stowasser, G., Tarling, G.A., Murphy, E.J., 2014. Interannual variability in Antarctic krill (*Euphausia superba*) density at South Georgia, Southern Ocean: 1997-2013. ICES J. Mar. Sci. 71, 2578-2588.

Flynn, A.J., Williams, A., 2012. Lanternfish (Pisces: Myctophidae) biomass distribution and oceanographic-topographic associations at Macquarie Island, Southern Ocean. Mar. Freshwater Res. 63, 251-263.

Foote, K.G., Knudsen, H.P., Vestnes, G., MacLennan, D.N., Simmonds, E.J., 1987. Calibration of acoustic instruments for fish density estimation: a practical guide. ICES Coop. Res. Rep. 144, 1-69.

Godø, O.R., Samuelsen, A., Macaulay, G.J., Patel, R., Hjøllo, S.S., Horne, J., Kaartvedt, S., Johannessen, J.A., 2012. Mesoscale eddies are oases for higher trophic marine life. PLoS ONE 7, e30161.

Greenlaw, C.F., 1977. Backscattering spectra of preserved zooplankton. J. Acoust. Soc. Am. 62, 44–52.

Guinet, C., Cherel, Y., Ridoux, V., Jouventin, P., 1996. Consumption of marine resources by seabirds and seals in Crozet and Kerguelen waters: changes in relation to consumer biomass 1962-85. Antarct. Sci. 8, 23-30.

Hamame, M., Antezana, T., 2010. Vertical diel migration and feeding of *Euphausia vallentini* within southern Chilean fjords. Deep-Sea Res. II 57, 642-651.

Handegard, N.O., du Buisson, L., Brehmer, P., Chalmers, S.J., De Robertis, A., Huse, G., Kloser, R., Macaulay, G., Maury, O., Ressler, P.H., Stenseth, N.C., Godø, O.R., 2013. Towards an acoustic-based coupled observation and modelling system for monitoring and predicting ecosystem dynamics of the open ocean. Fish Fish. 14, 605-615.

Hays, G.C., 2003. A review of the adaptive significanceand ecosystem consequences of zooplankton diet vertical migrations. Hydrobiologia 503, 163-170.

Holliday, D.V., Pieper, R.E., 1980. Volume scattering strengths and zooplankton distributions at acoustic frequencies between 0.5 and 3 MHz. J. Acoust. Soc. Am. 67, 135–146.

Hulley, P.A., Lutjeharms, J.R.E., 1995. The south-western limit for the warm-water, mesopelagic ichthyofauna of the Indo-West-Pacific: lanternfish (Myctophidae) as a case study. S. Afr. J. Mar. Sci., 15, 185-205.

Hunt, B.P.V., Pakhomov, E.A., Williams, R., 2011. Comparative analysis of the 1980s and 2004 macrozooplankton composition and distribution in the vicinity of Kerguelen and Heard Islands: seasonal cycles and oceanographic forcing of long-term change, in: Duhamel, G., Welsford, D. (Eds.) The Kerguelen Plateau: marine ecosystem and fisheries. Société Française d'Ichtyologie, Paris, pp. 79-92.

Irigoien, X., Klevjer, T.A., Røstad, A., Martinez, U., Boyra, G., Acuna, J.L., Bode, A., Echevarria, F., Gonzalez-Gordillo, J.I., Hernandez-Leon, S., Agusti, S., Aksnes, D.L., Duarte, C.M., Kaartvedt, S., 2014. Large mesopelagic fishes biomass and trophic efficiency in the open ocean. Nature Comm. 5, 3271.

Kaartvedt, S., Staby, A., Aksnes, D.L., 2012. Efficient trawl avoidance by mesopelagic fishes causes large underestimation of their biomass. Mar. Ecol. Prog. Ser. 456, 1–6.

Kang, M., Furusawa, M., Miyashita, K., 2002. Effective and accurate use of difference in mean volume backscattering strength to identify fish and plankton. ICES J. Mar. Sci. 59, 794–804.

Klevjer, T. A., Irigoien, X., Røstad, A., Fraile-Nuez, E., Benítez-Barrios, V. M., Kaartvedt,. S., 2016. Large scale patterns in vertical distribution and behaviour of mesopelagic scattering layers. Scientific Reports, 6, 19873.

Koizumi, K., Hiratsuka, S., Saito, H., 2014. Lipid and fatty acids of three edible myctophids, Diaphus watasei, Diaphus suborbitalis, and Benthosema pterotum: high levels of icosapentaenoic and docosahexaenoic acids. J. Oleo Sci. 63, 461-470.

Kloser, R.J., Ryan, T., Sakov, P., Williams, A., Koslow, J.A., 2002. Species identification in deep water using multiple acoustic frequencies. Can. J. Fish. Aquat. Sci. 59, 1065–1077.

Kloser, R.J., Ryan T.E., Young, J.W., Lewis, M.E., 2009. Acoustic observations of micronekton fish on the scale of an ocean basin: potential and challenges. ICES J. Mar. Sci. 66, 998-1006.

Korneliussen, R.J., Ona, E., 2003. Synthetic echograms generated from the relative frequency response. ICES J. Mar. Sci. 60, 636–640.

Koubbi, P., Moteki, M., Duhamel, G., Goarant, A., Hulley, P.A., O'Driscoll, R., Ishimaru, T., Pruvost, P., Tavernier, E., Hosie, G., 2011. Ecoregionalization of myctophid fish in the Indian sector of the Southern Ocean: results from generalized dissimilarity models. Deep-Sea Res. II 58, 170-180.

Lavery, A.C., Stanton, T.K., McGehee, D.E., Chu, D., 2002. Three-dimensional modeling of acoustic backscattering from fluid-like zooplankton. J. Acoust. Soc. Am. 111, 1197-1210.

Lawson, G.L., Wiebe, P.H., Stanton, T.K., Ashjian, C.J., 2008. Euphausiid distribution along the Western Antarctic Peninsula. Part A: development of robust multi-frequency acoustic techniques to identify euphausiid aggregations and quantify euphausiid size, abundance, and biomass. Deep-Sea Res. II 55, 412-431.

Lea, M.A., Cherel, Y., Guinet, C., Nichols, P.D., 2002. Antarctic fur seals foraging in the Polar Frontal Zone: inter-annual shifts in diet as shown from fecal and fatty acid analyses. Mar. Ecol. Prog. Ser. 245, 281-297 [Erratum in Mar. Ecol. Prog. Ser. 253, 310, 2003].

Lea, M.A., Guinet, C., Cherel, Y., Duhamel, G., Dubroca, L., Pruvost, P., Hindell, M., 2006. Impacts of climatic anomalies on provisioning strategies of a Southern Ocean predator. Mar. Ecol. Prog. Ser. 310, 77-94.

Lebourges-Dhaussy, A., Marchal, E., Menkès, C., Champalbert, G., Biessy, B., 2000. *Vinciguerria nimbaria* (micronekton), environment and tuna: their relationships in the Eastern Tropical Atlantic. Oceanol. Acta 23, 515–528.

Legendre, P., Fortin, M.J., 2004. Spatial pattern and ecological analysis. Vegetation 80, 107-138.

MacLennan, D.N., Fernandes, P.G., Dalen, J., 2002. A consistent approach to definitions and symbols in fisheries acoustics. ICES J. Mar. Sci. 59, 365-369.

Madureira, L.S.P., Everson, I., Murphy, E.J., 1993a. Interpretation of acoustic data at two frequencies to discriminate between Antarctic krill (*Euphausia superba* Dana) and other scatterers. J. Plankton Res. 15, 787-802.

Madureira, L.S.P., Ward, P., Atkinson, A., 1993b. Differences in backscattering strength determined at 120 and 38 kHz for three species of Antarctic macroplankton. Mar. Ecol. Prog. Ser. 93, 17-24.

Margalef, R., 1979. The organization of space. Oikos 33, 152-159.

Marshall, N.B., 1960. Swimbladder structure of deep-sea fishes in relation to their systematics and biology. Discovery Rep. XXXI, 1-122.

MATLAB 7.11.0.584, Release 2010b, The MathWorks, Inc., Natick, Massachusetts, United States.

Meillat, M., 2012. Essais du chalut mésopélagos pour le programme MYCTO 3D - MAP de l'IRD, à bord du Marion Dufresne (du 10 au 21 août 2012). Rapport de mission, Ifremer.

Miller, D.G.M., 1982. Results of a combined hydroacoustic and midwater trawling survey of the Prince Edward Island group. S. Afr. J. Antarct. Res. 12, 3-22.

Nicol, S., Foster, J., Kawaguchi, S., 2012. The fishery for Antarctic krill – recent developments. Fish Fish. 13, 30-40.

Pakhomov, E.A., Perissinotto, R., McQuaid, C.D., 1994. Comparative structure of the macrozooplankton/micronekton communities of the Subtropical and Antarctic Polar Fronts. Mar. Ecol. Prog. Ser. 111, 155-169.

Pakhomov, E.A., Perissinotto, R., McQuaid, C.D., 1996. Prey composition and daily rations of myctophid fishes in the Southern Ocean. Mar. Ecol. Prog. Ser. 134, 1-14.

Pakhomov, E.A., Froneman, P.W., 1999. Macroplankton/micronekton dynamics in the vicinity of the Prince Edward Islands (Southern Ocean). Mar. Biol. 134, 501-515.

Pakhomov, E.A., Froneman, P.W., 2000. Composition and spatial variability of macroplankton and micronekton within the Antarctic Polar Frontal Zone of the Indian Ocean during austral autumn 1997. Polar Biol. 23, 410-419.

Pakhomov, E., Yamamura, O., 2010. Report of the advisory panel on micronekton sampling inter-calibration experiment. PICES Scient. Rep. 38, 1-108.

Pauly, D., Christensen, V., Dalsgaard, J., Froese, R., Torres Jr, F., 1998. Fishing down marine food webs. Science 279, 860–863.

Perissinotto, R., McQuaid, C.D., 1992. Land-based predator impact on vertically migrating zooplankton and micronekton advected to a Southern Ocean archipelago. Mar. Ecol. Prog. Ser. 80, 15-27.

Potier, M., Marsac, F., Cherel, Y., Lucas, V., Sabatié, R., Maury, O., Ménard, F., 2007. Forage fauna in the diet of three large pelagic fishes (lancetfish, swordfish and yellowfin tuna) in the western equatorial Indian Ocean. Fish. Res. 83, 60-72.

R Core Team, 2014. R: a language and environment for statistical computing. R Foundation for Statistical Computing, Vienna, Austria. URL http://www.R-project.org/.

Ressler, P.H., Dalpadado, P., Macaulay, G.J., Handegard, N., Skern-Mauritzen, M., 2015. Acoustic surveys of euphausiids and models of baleen whale distribution in the Barents Sea. Mar. Ecol. Prog. Ser. 527, 13-29.

Ridoux, V., 1988. Subantarctic krill, *Euphausia vallentini* Stebbing, preyed upon by penguins around Crozet Islands (Southern Indian Ocean): population structure and annual cycle. J. Plankton Res. 10, 675-690.

Robertson, K.M., Chivers, S.J., 1997. Prey occurrence in pantropical spotted dolphins, Stenella attenuata, from the eastern tropical Pacific. Fish. Bull., 95, 334-348.

Rodhouse, P.G., Nigmatullin, C.M., 1996. Role as consumers. Phil. Trans. R. Soc. Lond. 351, 1003-1022.

Rodhouse, P.G., White, M.G., 1995. Cephalopods occupy the ecological niche of epipelagic fish in the Antarctic Polar Frontal Zone. Biol. Bull. 189, 77-80.

Sato, K., Charrassin, J.B., Bost, C.A., Naito, Y., 2004. Why do macaroni penguins choose shallow body angles that result in longer descent and ascent durations? J. Exp. Biol. 207, 4057-4065.

Saunders, R.A., Fielding, S., Thorpe, S.E., Tarling, G.A., 2013. School characteristics of mesopelagic fish at South Georgia. Deep Sea Res. I 81, 62–77.

Shaviklo, A.R., Rafipour, F., 2013. Surimi and surimi seafood from whole ungutted myctophid mince. LWT-Food Sci. Technol. 54, 463–468.

Simmonds, E.J., MacLennan, D.N., 2005. Fisheries acoustics: theory and practice. Second ed., Wiley-Blackwell, Oxford, UK.

Spear, L.B., Ainley, D.G., Walker, W.A., 2007. Foraging dynamics of seabirds in the eastern tropical Pacific Ocean. Studies Avian Biol. 35, 1-99.

Stanton, T.K., Wiebe, P.H., Chu, D., Benfield, M.C., Scanlon, L., Martin, L., Eastwood, R.L., 1994. On acoustic estimates of zooplankton biomass. ICES J. Mar. Sci. 51, 505-512.

Stanton, T.K., Chu, D., Wiebe, P.H., Martin, L., Eastwood, R.L., 1998a. Sound scattering by several zooplankton groups. I. Experimental determination of dominant scattering mechanisms. J. Acoust. Soc. Am. 103, 225–235.

Stanton, T.K., Chu, D., Wiebe, P.H., 1998b. Sound scattering by several zooplankton groups. II. Scattering models. J. Acoust. Soc. Am. 103, 236–254.

Stanton, T.K., Chu, D., 2000. Review and recommendations for the modelling of acoustic scattering by fluid-like elongated zooplankton: euphausiids and copepods. ICES J. Mar. Sci. 57, 793–807.

Sund, O., 1935. Echo sounding in fishery research. Nature 135, 953.

Tremblay, Y., Cherel, Y., 2003. Geographic variation in the foraging behaviour, diet and chick growth of rockhopper penguins. Mar. Ecol. Prog. Ser. 251, 279-297.

Warren, J.D., Stanton, T.K., Benfield, M.C., Wiebe, P.H., Chu, D., Sutor, M., 2001. In situ measurements of acoustic target strengths of gas-bearing siphonophores. ICES J. Mar. Sci. 58, 740–749.

Wiebe, P.H., Chu, D., Kaartvedt, S., Hundt, A., Melle, W., Ona, E., Batta-Lona, P., 2010. The acoustic properties of *Salpa thompsoni*. ICES J. Mar. Sci. 67, 583-593.

Williams, A., and Koslow, J.A. 1997. Species composition, biomass and vertical distribution of micronekton over the mid-slope region off southern Tasmania. Mar. Biol. 130, 259–276.

Woehler, E.J., Green, K., 1992. Consumption of marine resources by seabirds and seals at Heard Island and the McDonald Islands. Polar Biol.12, 659-665.

Ye, Z., 1997. Low-frequency acoustic scattering by gas-filled prolate spheroids in liquids. J. Acoust. Soc. Am. 101, 1945-1952.

Fig. 1. 38 and 120 kHz echograms representing acoustic density (in color, S_v in dB) recorded on the 24th of January 2014 morning from 30 to 300m depth in east waters off Kerguelen.

Fig. 2. Schematic description of the relative frequency response, r(f). Horizontal lines indicate typical range positions of selected acoustic categories when measured at frequencies 18-200 kHz. Source: Korneliussen and Ona (2003).

Fig. 3. Acoustic records and the corresponding cruise trawls (T07 and T14) that were used to define thresholds of difference in the bi-frequency algorithm. Upper panel: complete trawl echograms with trawling depths (continuous black line) and limits of data extraction (dashed black lines). Lower panel: extracted echogram samples focusing on the trawl targeted aggregates that were selected from acoustic identification estimation. Left: T07 trawl (euphausiids) sampling on the 120 kHz frequency to discriminate the “fluid-like” group. Right: T14 trawl (gas-filled swimbladder fish) on the 38 kHz frequency to discriminate the “gas-bearing” group.

Fig. 4. Left panel (a): frequency response of each sample considered relatively to the 38 kHz frequency, with "fluid-like" samples (from the trawl T07) represented in red and "gas-bearing" samples (from the trawl T14) in blue. Right panel (b): bar chart of the percentage of "fluid-like" (in red) and "gas-bearing" (in blue) total NASC, according to a -15 to 25 dB range of threshold of difference, used to define the best thresholds (-1 and +2 dB) delimiting the “undetermined” group by transferring a maximum of 10% of their acoustic energy (total NASC).

Fig. 5. Summary diagram of the bi-frequency algorithm method used in this study.

Fig. 6. Representative diagram of the number of patches (in blue) and its derivative (in green) detected along increasing S_v values from -70 to -40 dB. The value of -63 dB corresponds to a threshold level over which the number of patches did not further increased.

Fig. 7. 38 and 120 kHz echograms representing acoustic density (in color, S_v in dB) recorded on the 24th of January 2014 morning from 30 to 300m depth in east waters off Kerguelen for (a) patches- and (b) layers structures.

Fig. 8. Total density (NASC, in $m^2 \cdot nmi^{-2}$, colored on ship track) integrated from 30 to 300 m depth for each acoustic group ("gas-bearing", fluid-like" and "undetermined" groups) and for each type of structures (patches and layers).

Fig. 9. Mean vertical NASC profiles from 30 to 300 m depth of each acoustic group ("gas-bearing", fluid-like" and "undetermined" groups) for day (black lines) and night (grey lines) and for each type of structures (patches and layers). Dashed lines indicate the 95% confidence intervals.